

TNO PUBLIEK

Westerduinweg 3 1755 LE Petten P.O. Box 15 1755 ZG Petten The Netherlands

www.tno.nl

T +31 88 866 50 65

TNO report

TNO 2021 R10039 | Final report

Uncertainty in fiber optic strain measurements for blade bending moments

Date 27 January 2021

Author(s) J.W. Wagenaar, P.A. vd Werff, F.A. Kaandorp

Copy no. No. of copies

Number of pages 18 Number of appendices 2

Customer TNO Wind Energy

Project name TKI HER GE Haliade X Demo: Fiber optic uncertainty

Project number 060.34375

All rights reserved.

No part of this publication may be reproduced and/or published by print, photoprint, microfilm or any other means without the previous written consent of TNO.

In case this report was drafted on instructions, the rights and obligations of contracting parties are subject to either the General Terms and Conditions for commissions to TNO, or the relevant agreement concluded between the contracting parties. Submitting the report for inspection to parties who have a direct interest is permitted.

© 2021 TNO

Contents

Execu	utive Summary	3
1	Introduction	4
2	Fiber optic technologies	5
2.1	Classical, fiber optic strain sensor	5
2.2	Temperature calibrated fiber optic sensor	
2.3	Stud mounted FOBM sensor	6
3	Relation to electrical strain gauges	7
4	Mounting	9
5	Uncertainty calculation	10
Refere	rences	14
Apper	ndix A: Derivation	15
Apper	ndix B: Sensitivity factors	17

Executive Summary

Recently, fiber optic strain measurements are being used for blade bending moment measurements to larger extents. Hence, this report describes a general mathematical model for fiber optic strain and blade bending moments. It allows for a complete overview and relation between all relevant uncertainties specified for the two presented fiber optics measurement principles: (temperature calibrated) pad mounted and stud mounted. The latter is referred to as the fiber optic blade monitoring FOBM sensor.

The way in which the sensors are mounted to the blades plays an important role as there is some response attenuation between the strain transfer from the specimen to the strain sensor. We believe that because of the glue layer, the response attenuation for pad mounted sensors is higher than for stud mounted sensors. That means that, if we ignore uncertainty, the FOBM is better able to represent the **strain** in blades than (temperature calibrated) pad mounted fiber optic sensors. Typically, we estimate this effect to be 2%.

However, as long as response attenuation is linear and constant in time this effect can easily be taken up in the calibration coefficient expressing the relation between strain and blade bending moments. Hence, this response attenuation is irrelevant for blade bending moments, meaning that, given this set-up and not considering uncertainty, pad mounted sensors and the FOBM sensor can equally well represent blade bending **moments**.

From the uncertainty budgets we see that the uncertainties of the pad-mounted sensor and the FOBM sensor are about the same: 35,11 $\mu\epsilon$ / 4,2% and 35,62 $\mu\epsilon$ / 4,3%, respectively, where the uncertainty of the pad-mounted sensor is just a little bit lower. We also see that in both cases the largest contribution comes from the uncertainty related to the blade temperature expansion coefficient.

1 Introduction

In wind turbine validation measurements, we are interested in understanding the structural behaviour of wind turbine blades. Among this, we are interested in knowing the blade (root) bending moments.

For these measurements we can use either electrical strain gauges or fiber optic strain gauges. For many years TNO Wind Energy (formerly known as ECN Wind Energy) has been using electrical strain gauges and their working principle is well understood and documented. This also applies to uncertainties related to electrical strain gauge based blade bending moment measurements. See [1].

Recently, fiber optic strain measurements are being used for blade bending moment measurements to larger extents. Here, different suppliers provide various fiber optic strain sensors. We distinguish between fibers that are directly glued to the surface in a 'pad'-kind of manner and fibers that are fixed on a sensor body that is subsequently mounted on the surface using the ECN patented stud method [2]. Advantage of this latter system is that the sensor can separately be calibrated, it measures over a certain range (studs are about 10cm apart) and it can easily be removed, replaced and even reused. A validation of this fiber optic blade monitoring (FOBM) sensor was done through a field campaign [3].

Besides the measurement principle itself, we want to quantify its uncertainty. Hence, this report describes a general mathematical model for fiber optic strain and blade bending moment measurements. It allows for complete overview and relation between all relevant uncertainties specified for the two presented fiber optics measurement principles: pad mounted and stud mounted. 'Pad mounted' is referred to as the 'classical' way.

In the framework of blade bending moments, we present in chapter 2 the various fiber optic technologies in some more detail. Next, we present the resemblance with electrical strain gauge based blade bending moments in chapter 3; after all, they aim to measure the same quantity. The effect of the mounting is detailed in chapter 4 and last but not least, we present the actual uncertainty budget in chapter 5.

2 Fiber optic technologies

In blade measurements we want to know the edgewise and flatwise bending moments M_e and M_f , respectively. As such we measure the strain in the edgewise and flatwise direction (ϵ_e and ϵ_f , respectively) and we allow for cross talk between the strain directions in obtaining the bending moments. Traditionally, and mimicking [1], this results in the following matrix relation between bending moments and strains:

$$M = G^{fo} * (\varepsilon_X - O^{fo}), \tag{1}$$

with

$$M = {M_e \choose M_f},$$

$$G^{fo} = {G_{11}^{fo} G_{12}^{fo} \choose G_{21}^{fo} G_{22}^{fo}}$$

$$\varepsilon_X = {\varepsilon_e \choose \varepsilon_f}$$

$$O^{fo} = {O_e^{fo} \choose O_f^{fo}}.$$
(2)

Here, G^{fo} is the gain matrix and O^{fo} is the offset. We have added an additional 'fo' superscript (short for 'fiber optic') in order not to assume that this equation generally holds. We will return to this generality later on.

With respect to the strain measurements, we assume that strains and temperatures are measured with fiber optic sensors at the leading edge (LE), trailing edge (TE), upwind (UW) and downwind (DW) side of a wind turbine blade. For simplicity, we assume for now that these measurement take place in the blade root. Therefore, we have the following relations:

$$\varepsilon_e = \varepsilon_{TE} - \varepsilon_{LE}
\varepsilon_f = \varepsilon_{UW} - \varepsilon_{DW}.$$
(3)

2.1 Classical, fiber optic strain sensor

As said, the measurements are performed with fiber optic sensors and according to [4] the relation between strain (ϵ_{xx}) and the fiber optic strain measurement ($\lambda_{\epsilon,xx}$), temperature compensated with a fiber optic temperature measurement ($\lambda_{T,xx}$) is as follows:

$$\varepsilon_{xx} = \frac{1}{k} \frac{\Delta \lambda_{\varepsilon,xx}}{\lambda_{0\varepsilon,xx}} - \frac{1}{k} \frac{\Delta \lambda_{T,xx}}{\lambda_{0T,xx}} \left(\frac{k \alpha_{sp} + \alpha_{\delta}}{k \alpha_{gl} + \alpha_{\delta}} \right) \qquad (\alpha_{\delta} >> k \alpha_{gl})$$

$$\varepsilon_{xx} \approx \frac{1}{k} \frac{\Delta \lambda_{\varepsilon,xx}}{\lambda_{0\varepsilon,xx}} - \frac{1}{k} \frac{\Delta \lambda_{T,xx}}{\lambda_{0T,xx}} \left(\frac{k \alpha_{sp}}{\alpha_{\delta}} + 1 \right),$$
(4)

where xx is either LE, TE, UW, DW. Furthermore and following [4],

 $\lambda_{0\epsilon,T}$ = base wavelength or peak wavelength of the undisturbed grating of the fiber optic strain sensor ϵ or temperature sensor T.

 $\Delta\lambda_{\epsilon,T}$ = difference in base wavelength from the shifted wavelength of the disturbed grating resulting from the experienced strain ϵ or temperature T.

k = gauge factor. Also defined as k = 1-p, where p is the photo-elastic coefficient α_{gl} = expansion coefficient of the glass fiber. As explained in Annex A, this will further be neglected.

 α_{sp} = expansion coefficient of the specimen

 α_{δ} = change of refraction index.

2.2 Temperature calibrated fiber optic sensor

In many cases the fiber optic temperature sensor is a separate sensor. Moreover, it can separately be calibrated as for instance the case in HBM sensors (an example is presented in [5]). We consider this option in our set-up and assume the measured strain is a combination of a fiber optic strain sensor and a calibrated, fiber optic temperature sensor. In that case equation (4) reads

$$\varepsilon_{xx} = \frac{1}{k} \frac{\Delta \lambda_{\varepsilon,xx}}{\lambda_{0\varepsilon,xx}} - \frac{1}{k} \Delta T (k \alpha_{sp} + \alpha_{\delta}), \tag{5}$$

where ΔT is the temperature change. From now on, we will consider temperature calibrated fiber optic sensors in our analyses.

2.3 Stud mounted FOBM sensor

Equation (4) holds in general and for the specific case of a Fiber Optic Blade Monitoring (FOBM) sensor with stud mounting, we proof in appendix A that the following equation holds

$$\varepsilon_{xx} = \frac{1}{k} \frac{\Delta \lambda_{\varepsilon,xx}}{\lambda_{0\varepsilon,xx}} - \frac{1}{k} \frac{\Delta \lambda_{T,xx}}{\lambda_{0T,xx}} \left(\frac{k\alpha_{sp} + \alpha_{\delta} + k\alpha_{ss} \frac{S}{W}}{k\alpha_{ss} + \alpha_{\delta}} \right), \tag{6}$$

where, in addition to the above

 α_{ss} = expansion coefficient of stainless steel (carrier of the fibers in the FOBM sensor) S = width of the FOBM stud

W = distance between fixation points.

Going back to equation (1), we can now see that in determining the moments there are parts that arise from the calibration (G^{fo} and O^{fo}) and a part that arises from the sensoring (ε_x). This split-up between calibration and sensoring is also important in the uncertainty quantification.

$$M = G^{fo} * (arepsilon_X - O^{fo})$$

Looking at equation (4) one might have chosen to 'move' some of the constants to the gain-factors and make them part of the calibration. However, this form seems easier to deal with and resembles the electrical strain gauge case which we will consider, next.

3 Relation to electrical strain gauges

When using electrical strain gauges in determining the blade moments, one is addressing the same quantity. According to [1] the relation between the blade bending moments (M) and the measured signals (S) is:

$$M = G^{el} * (S_X - O^{el}), \tag{7}$$

where M is defined in (2). Similar to (2), G^{el} is the gain matrix and O^{el} is the offset, where the superscript 'el' now stands for 'electric'. Furthermore, signal $S_x = {S_e \choose S_e}$.

According to [1], S_x arises from an applied voltage (V) and a resulting voltage (V_0) from a blade measurement bridge configuration. The (disturbed) strains from the strain sensors, which are resistance based, result in a varied returned voltage. In formula form, for both edgewise (e) and flatwise (f) this reads:

$$S_X \stackrel{\text{def}}{=} \frac{V_0}{V}, \, \mathbf{x} = \mathbf{e} \text{ or f}$$
 (8)
 $V_0 = \frac{k^{el}}{4} (\varepsilon_1 - \varepsilon_2 + \varepsilon_3 - \varepsilon_4) V,$

where k^{el} results from the relation between the experienced strain (ε) and an electrical resistance based strain gauge sensor (see [6] for more details).

Next, we assume that we use for both edgewise and flatwise strain, two parallel strain gauges in a full bridge configuration. If we neglect, for the sake of clarity, small differences between the various strain installations and measurements and assume an ideal case, we obtain the following relations

$$\varepsilon_{1} = \varepsilon_{X} = -\varepsilon_{2}; \varepsilon_{3} = \varepsilon_{X} = -\varepsilon_{4}$$

$$V_{0} = k^{el} \varepsilon V$$

$$S_{X} = k^{el} \varepsilon_{X}.$$
(9)

Having obtained this, we can equate and compare (1) and (7):

$$M = G^{fo} * (\varepsilon_X - O^{fo}) = G^{el} * (S_X - O^{el})$$

$$= G^{el} * (k^{el} \varepsilon_X - O^{el})$$

$$= \frac{G^{el}}{k^{el}} * (\varepsilon_X - k^{el} O^{el}).$$
(10)

From this, we can deduce that

$$G^{fo} = \frac{G^{el}}{k^{el}}$$

$$O^{fo} = k^{el}O^{el}.$$
(11)

Here, we have obtained a relation between the calibration factors resulting from calibrating two full bridge configurations with pairs of parallel electrical strain gauges and a sequence of four fiber optic strain (and temperature) measurements at the LE, TE, UW and DW side. Of course, relations (11) are obtained under ideal circumstances, but can perfectly serve as a plausibility check.

Nevertheless, when adding the details of the various sensors in equation (11), it will provide us the means to not only compare the calibration, but also the uncertainty budgets, in a consistent manner.

4 Mounting

Fiber optic sensors are mounted to the specimen of which they measure the strain; in our case blades. This mounting may have an effect on the strain measurement and we want to take that into account.

Fiber optic sensors are usually mounted to the specimen using some kind of glue and in the case of the FOBM sensors studs are being used. In this latter case, the studs are glued to the blade.

Finite Element Model (FEM) studies [7] have shown that there is some response attenuation between the strain transfer from the specimen to the strain sensor. Typically, this is a fixed linear response and so we allow in (1) for a close-to-one constant factor between bending moment M and measured strain ϵ

$$M = G^{fo} * (\varepsilon_{C,X} - O^{fo})$$

$$\varepsilon_{C,X} = C * \varepsilon_{X},$$
(12)

where

C = Coefficient quantifying the response lag between the strain transfer from the specimen to the strain sensor. Typically, it is a close-to-one constant factor. ε_x is defined in (4), (5) or (6) (through (3)).

Here, based on the FEM analysis of [7] we estimate the following values for this coefficient

C = 0.98 for pad mounted

• C = 0.9987 for stud mounted

In both cases, we assume the uncertainty to be 0.

We believe that because of the glue layer, the C coefficient for pad mounted sensors is less (or less known) than for stud mounted sensors, i.e. the C coefficient for stud mounted sensors is closer to 1. This means that, not considering uncertainty, the FOBM sensor is better able to represent the strain in blades than pad mounted fiber optic sensors by an amount of almost 2%.

However, as long as the C coefficient is linear and constant in time this effect can easily be taken up in the calibration coefficient G^{fo} and hence it is irrelevant for blade bending moments. This means that, given this set-up and not considering uncertainty, pad mounted sensors and the FOBM sensor can equally well represent blade bending moments.

5 Uncertainty calculation

For the uncertainty calculation in fiber optic measured blade bending moments, we consider the following mathematical model, based on (1):

$$M = (G^{fo} + \delta G_T) * (\varepsilon_{C,X} + \delta \varepsilon_{\varepsilon T} + \delta \varepsilon_{RH} - O^{fo}) , \qquad (13)$$

where

 δG_T = temperature dependence on gain G

 $\delta \epsilon_{\rm ET}$ = uncertainty related to the fact that the strain sensor and the temperature sensor are not measuring exactly at the same spot. Also, the blade material has some thickness and strain already occurs due to penetrating temperature. While the changing temperature has not reached sensor, yet, strain is already being detected. Hence, there is a time lag in the temperature sensing.

 $\delta \epsilon_{RH}$ = effect of relative humidity on strain/temperature sensing.

Very similar to [1], the gain matrix G^{fo} and the offset O^{fo} result from the calibration procedure using the blade's own weight as reference. Particularly, the uncertainty in gain matrix G^{fo} results from the uncertainty in the underlying fit parameters A_{ij} (type A) and a Monte Carlo simulation on the various input parameter in the reference load (type B). Again, the procedure is exactly the same as outlined in [1], where we take care of small difference therein, elaborated in equation (11), above.

Sensing uncertainty is taken care off through equation (4), where we assume uncertainty contributions from constants therein: u_k , $u_{\alpha sp}$, $u_{\alpha \delta}$. Furthermore, we assume uncertainty in the returned, shifted wavelength ($\Delta \lambda_{\epsilon,T}$) as the result from the interrogator that reads it out:

$$u_{\Delta\lambda_{\varepsilon T}}^2 = u_{int_{\varepsilon T}}^2,\tag{14}$$

where the subscripts ϵ and T refer to the fiber optic strain sensor and temperature sensor, respectively, and the interrogator that reads them out. We realize that in many cases it will be the same interrogator that does so, but that does not in general need to be the case.

Last, but not least and similar to [1], we allow for so-called ' δ '-terms in equation (13). They do not contribute in determining the moment (values are zero), but they do in the uncertainty budget. We have chosen to add one term (δG_T) to the calibration part and two terms ($\delta \epsilon_{\epsilon T} + \delta \epsilon_{RH}$) to the 'sensor' part in equation (13). For simplicity reasons, we will consider these sensor part ' δ '-terms to be equal (in uncertainty) for both edgewise and flatwise direction, although equation (13) could easily allow for distinguishing between the two in a vector-like notation. We realize that equation (13) does not allow for different ' δ '-term (uncertainty) values for the stress sensor and the temperature sensor, separately, which we take for granted.

Also, we note that equation (13), as compared to [1], does not include a term, which should account for the fact that the electric wires connecting the electrical strain gauges have resistance as well impacting the strain measurements. Obviously, fiber optics do not suffer from this. They might suffer from polarization in the fiber due to

bending or twist, which may influence the detection. However, our current interrogators are insensitive to this effect.

With the above, we have completed our mathematical model for the uncertainty calculation and we can start the calculation itself

$$u_{M}^{2} = u_{M,calib}^{2} + u_{M,sens}^{2}$$

$$u_{M,calib}^{2} = \left(\frac{\partial M}{\partial A}\right)^{2} u_{A}^{2} + \left(\frac{\partial M}{\partial \delta G_{T}}\right)^{2} u_{\delta G_{T}}^{2} + u_{M,ref}^{2}$$

$$u_{M,sens}^{2} = \sum_{i,j} \left(\frac{\partial M}{\partial c_{i}}\right) \left(\frac{\partial M}{\partial c_{j}}\right) u_{c_{i}} u_{c_{j}} \rho_{ij},$$

$$(15)$$

where $c_i = (\Delta\lambda_{\epsilon,LE}, \Delta\lambda_{\epsilon,TE}, \Delta\lambda_{\epsilon,DW}, \Delta\lambda_{\epsilon,DW}, \Delta T_{LE}, \Delta T_{TE}, \Delta T_{DW}, \Delta T_{DW}, k, \alpha_{sp}, \alpha_{\delta}, \delta\epsilon_{\epsilon T}, \delta\epsilon_{RH})$ in case of the temperature calibrated fiber optic sensor and $c_i = (\Delta\lambda_{\epsilon,LE}, \Delta\lambda_{\epsilon,TE}, \Delta\lambda_{\epsilon,DW}, \Delta\lambda_{T,LE}, \Delta\lambda_{T,TE}, \Delta\lambda_{T,DW}, \Delta\lambda_{T,DW}, k, \alpha_{sp}, \alpha_{\delta}, \alpha_{ss}, S, W, \delta\epsilon_{\epsilon T}, \delta\epsilon_{RH})$ in case of the stud mounted fiber optic sensor. Also, ρ_{ij} represents the correlation between uncertainty components u_i and u_j .

As stressed before, the uncertainty in the bending moment M comprises of a part that relates to the uncertainty in the calibration and an uncertainty in the sensoring. This is also reflected in (15). Realizing that the calibration provides a linear coefficient between moment M and strain ϵ (apart from the offset O), we rewrite the last line of (15) as:

$$u_{M,sens}^{2} = \sum_{i,j} \left(\frac{\partial M}{\partial c_{i}} \right) \left(\frac{\partial M}{\partial c_{j}} \right) u_{c_{i}} u_{c_{j}} \rho_{ij},$$

$$= G^{fo} \sum_{i,j} \left(\frac{\partial \varepsilon_{m}}{\partial c_{i}} \right) \left(\frac{\partial \varepsilon_{m}}{\partial c_{j}} \right) u_{c_{i}} u_{c_{j}} \rho_{ij}, \tag{16}$$

Where ci is defined as above.

Also because the calibration is a separate exercise with separate values and uncertainty contributions, we focus here on the uncertainty of the sensoring. The mathematical framework is provided in equation (13) and (16) and the sensitivity factors (partial derivatives of (16)) are provided in appendix B. The resulting uncertainty budgets are provided below as well as explanation about the reported numbers. In the uncertainty budgets we consider the correlation between uncertainty components to be zero ($\rho_{ij} = 1$, when i=j and $\rho_{ij} = 0$, otherwise).

Temperature calibrated, pad mounted FO

$$\varepsilon_{m} = \mathrm{C} * \left(\frac{1}{k} \frac{\Delta \lambda_{\varepsilon}}{\lambda_{0\varepsilon}} - \frac{1}{k} \Delta T \left(\alpha_{\delta} + k \; \alpha_{sp} \right) \right) + \delta \varepsilon_{RH} + \delta \varepsilon_{\varepsilon T}$$

quantity		estimate	expanded uncertainty	coverage factor	Probability distribution	standard uncertainty	sensitivity coefficient	uncertainty contribution	
X _i		Value _i	U	k		unc(x _i)			%
С	[-]	0,95	0,000	1	Normal	0,000	876,107	0,000	0,0%
$\Delta \lambda_{\epsilon}$	nm	1,60	0,014	1	Normal	0,014	791,660	11,083	10,0%
ΔΤ	К	30,000	0,500	1	Rectangular	0,289	-14,478	-4,180	1,4%
k	[-]	0,790	0,016	1	Rectangular	0,009	-1270,002	-11,585	10,9%
$\alpha_{\sf sp}$	με/Κ	6,00	1,00	1	Normal	1,000	-28,500	-28,500	65,9%
α_{δ}	με/К	7,30	0,10	1	Rectangular	0,058	-36,076	-2,083	0,4%
$\delta \epsilon_{\text{RH}}$	με ([-])	0,00	5,00	1	Rectangular	2,887	1,000	2,887	0,7%
$\delta\epsilon_{\text{eT}}$	με ([-])	0,00	20,00	1	Rectangular	11,547	1,000	11,547	10,8%
Ref: λ _{0ε}	nm	1519,00	0,00	1	Normal	0,000	0,834	0,000	
							ε _m	832,30168	με ([-])
							unc ɛm	35,111	με ([–])
							[%]	4,2%	

X _i	Unit	Value _i	Explanation	U	Explanation	
С	[-]	0,950	See document	0,000	See document	
$\Delta \lambda_{\epsilon}$	nm	1,600	Typical strain range	0,014	Uncertaint of interrogator	
ΔΤ	K	30,000	Typical temp range	0,500	see calibrationn sheet [5]	
k	[-]	0,790	See calibration sheet	0,016	2%; see calibration sheet [5]	
$lpha_{\sf sp}$	με/Κ	6,000	Typical value for blades	1,000	Engineering judgement	
α_{δ}	με/Κ	7,300	Typical value for type of fiber	0,100	Engineering judgement	
$\delta\epsilon_{\text{RH}}$	με ([–])	0,000		5,0	Engineering judgement	
$\delta\epsilon_{ ext{ iny ET}}$	με ([-])	0,000		20,0	Engineering judgement	
Ref: $\lambda_{0\epsilon}$	nm	1519,000	Typical reference wavelength	0,000		

FOBM

$$\varepsilon_{m} = C \left(\frac{1}{k} \frac{\Delta \lambda_{\varepsilon}}{\bar{\lambda}_{0\varepsilon}} - \frac{1}{k} \frac{\Delta \lambda_{T}}{\bar{\lambda}_{0T}} \left(\frac{k \alpha_{sp} + \alpha_{\delta} + \frac{S}{W} k \alpha_{ss}}{k \alpha_{ss} + \alpha_{\delta}} \right) \right) + \delta \varepsilon_{RH} + \delta \varepsilon_{\ell T}$$

quantity		estimate	expanded uncertainty	coverage factor	Probability distribution	standard uncertainty	sensitivity coefficient	uncertainty contribution	
		Value _i	U					u _i y	%
	[-]	0,980	0,000	1	Normal	0,000	853,32	0,00	0,0%
	nm	1,600	0,014	1	Normal	0,014	816,66	11,43	10,3%
	nm	0,900	0,014	1	Normal	0,014	-522,67	-7,32	4,2%
	[-]	0,790	0,016	1	Rectangular	0,009	-938,31	-8,56	5,8%
	με/Κ	6,000	1,000	1	Normal	1,000	-28,55	-28,55	64,3%
	με/К	7,300	0,100	1	Normal	0,100	-13,01	-1,30	0,1%
	με/К	16,500	0,165	1	Normal	0,165	16,14	2,66	0,6%
S	mm	8,000	0,010	1	Normal	0,010	-4,40	-0,04	0,0%
	mm	107,000	0,100	1	Normal	0,100	-0,33	-0,03	0,0%
	με ([-])	0,000	12,7	1	Rectangular	7,332	1,00	7,33	4,2%
	με ([-])	0,000	20,0	1	Rectangular	11,547	1,00	11,55	10,5%
	nm	1519,000	0,000	1	Normal	0,000	0,86	0,00	0,0%
Ref: λ_{0T}	nm	1519,000	0,000	1	Normal	0,000	0,29	0,00	0,0%
				·		, and the second	ε _m	836,25	με ([-])
							unc ɛm	35,62	με ([–])
							[%]	4,3%	

X _i	Unit	Value _i	Explanation	U	Explanation
С	[-]	0,980	See document	0,000	See document
$\Delta\lambda_{\epsilon}$	nm	1,600	Typical strain range	0,014	Uncertaint of interrogator
$\Delta \lambda_{ m T}$	nm	0,900	Typical temp range	0,014	Uncertaint of interrogator
k	[-]	0,790	See calibration sheet	0,016	2%; see calibration sheet [5]
$\alpha_{\sf sp}$	με/Κ	6,000	Typical value for blades	1,000	Engineering judgement
α_{δ}	με/Κ	7,300	Typical value for type of fiber	0,100	Engineering judgement
α_{ss}	με/Κ	16,500	Value for stainless steel	0,165	1%
S	mm	8,000	Exact dimension according to CAT	0,010	Precision of manufacturing
W	mm	107,000	Exact dimension according to CAT	0,100	Precision of mold
$\delta\epsilon_{\text{RH}}$	με ([–])	0,000		12,7	15nm; according to [8]
$\delta\epsilon_{ extsf{et}}$	με ([-])	0,000		20,0	Engineering judgement
Ref: $\lambda_{0\epsilon}$	nm	1519,000	Typical reference wavelength	0,000	
Ref: $\lambda_{0\mathrm{T}}$	nm	1519,000	Typical reference wavelength	0,000	

From the uncertainty budgets we see that with the given representative values (3rd column), the uncertainties of the pad-mounted sensor and the FOBM sensor are about the same: 35,11 $\mu\epsilon$ / 4,2% and 35,62 $\mu\epsilon$ / 4,3%, respectively, where the uncertainty of the pad-mounted sensor is just a little bit lower.

We also see that the uncertainty in the blade temperature expansion coefficient α_{sp} has the largest contribution to the uncertainty.

References

- [1] J.W. Wagenaar, P.A. vd Werff and H. Braam, 'Onzekerhede bij Mechanische Belastingen', ECN-Wind Memo-11-029, April 2011
- [2] T.W. Verbrugge, 'Device and method for measuring strain', WO 2010/117260 A1, 2003
- [3] F.A. Kaandorp, 'Completion report LoadWatch measurement campaign at N5', TNO 2019 R11595, October 2018 F.A. Kaandorp, 'Findings report of the measurements at the XEMC Darwind XD115 turbine in the framework of the LoadWatch TKI-WoZ R&D project', TNO
- [4] M. Kreuzer, 'Strain Measurement with Fiber Bragg Grating Sensors', S2338-1.0 en, HBM
- [5] J. Ribeiro, 'HBM FS63 Composite Temperature Sensor Calibration Sheet', K-SYS-FSS, 046 840 633 134-W, 26th June 2019.
- [6] Strain gauge Wikipedia, 6th January 2021

2019 R11594, October 2018

- [7] M. van der Hoek, 'White Paper: Analysis of various aspects of sensor fixation for accurate measurement of strain in blades of Wind Turbines' LoadWatch progress presentation, September 2019, updated January 2021.
- [8] M. vd Hoek, 'Calculation of Blade Strain from FOBM-sensor signal', presentation of LoadWatch project progress meeting, 18th of February 2018

Appendix A: Derivation

The fiber optic strain sensor FOBM experiences strain from a number of sources: the actual strain it is supposed to sense (Em), strain as the result of temperature change in the specimen, thermo-optical response of the grating, expansion of the stainless steel studs due to temperature change and strain as the result of relative humidity change. In fact, there is yet another term that should be taken into account, i.e. the expansion of the fiber itself due to temperature change (k α_{ql} ΔT). In [4], this is considered for the temperature sensor only, whereas we feel that is applies to the strain sensor as well. However, as stated in [4], this contribution is relative small and is from practical point of view taken together with the thermo-optical response of the grating as a combined temperature effect on the fiber including grating.

The strain in the FOBM sensor due to expansion of the stainless steel study resulting from temperature change is depicted in figure 1 (from [8]). Combining the various sources in formula form, reads:

$$\frac{\Delta \lambda_{\varepsilon}}{\lambda_{cs}} = k\varepsilon_m + k\alpha_{sp}\Delta T + \alpha_{\delta}\Delta T + k\alpha_{ss}\frac{s}{w}\Delta T + \alpha_{RH}\Delta RH \tag{A1a}$$

$$\frac{\Delta \lambda_{\varepsilon}}{\lambda_{0\varepsilon}} = k\varepsilon_{m} + k\alpha_{sp}\Delta T + \alpha_{\delta}\Delta T + k\alpha_{ss}\frac{s}{w}\Delta T + \alpha_{RH}\Delta RH$$
 (A1a)
$$\frac{\Delta \lambda_{\varepsilon}}{\lambda_{0\varepsilon}} = k\varepsilon_{m} + \left(k\alpha_{sp} + \alpha_{\delta} + k\alpha_{ss}\frac{s}{w}\right)\Delta T + \alpha_{RH}\Delta RH$$
 (A1b)

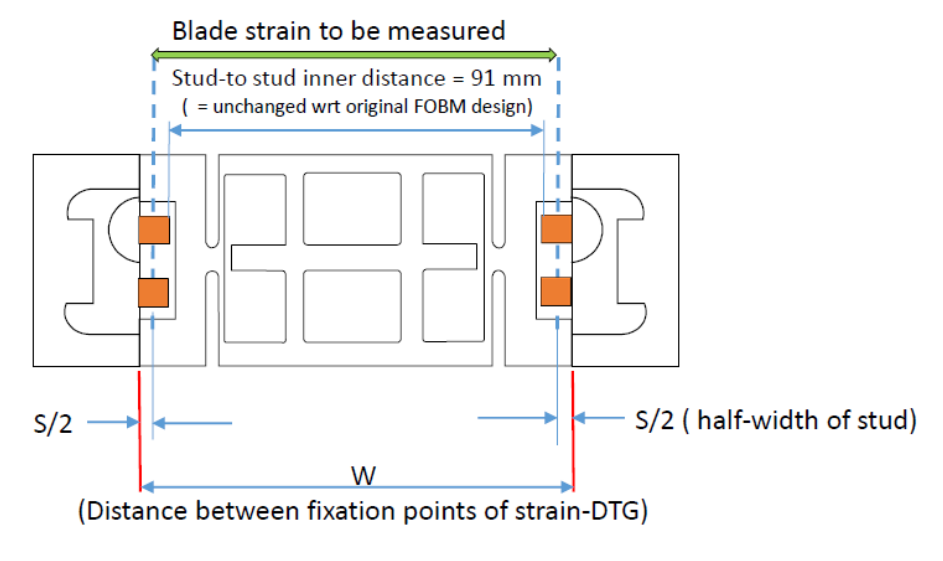


Figure 1: Schematic overview of FOBM sensor body with explicit focus on stud width S and the distances between the studs W. The figure is from [xx]

At the same time, the fiber optic temperature sensor in the same FOBM body, experiences strain from similar sources:

$$\frac{\Delta \lambda_T}{\lambda_{0T}} = k\alpha_{ss}\Delta T + \alpha_{\delta}\Delta T + \alpha_{RH}\Delta RH \tag{A2a}$$

$$\frac{\Delta \lambda_T}{\lambda_{0T}} = k\alpha_{SS}\Delta T + \alpha_{\delta}\Delta T + \alpha_{RH}\Delta RH$$

$$\Delta T = \frac{1}{k\alpha_{SS} + \alpha_{\delta}} \left(\frac{\Delta \lambda_T}{\lambda_{0T}} - \alpha_{RH}\Delta RH\right)$$
(A2a)
(A2b)

Method 1

Subtract (A2a) from (A1a)

$$\frac{\Delta \lambda_{\varepsilon}}{\lambda_{0\varepsilon}} - \frac{\Delta \lambda_{T}}{\lambda_{0T}} = k\varepsilon_{m} + k\alpha_{sp}\Delta T + k\alpha_{ss}\frac{s}{W}\Delta T - k\alpha_{ss}\Delta T \tag{A3}$$

Rearranging and using (A2b) yields

$$\varepsilon_{m} = \frac{1}{k} \frac{\Delta \lambda_{\varepsilon}}{\lambda_{0\varepsilon}} - \frac{1}{k} \frac{\Delta \lambda_{T}}{\lambda_{0T}} - \frac{\alpha_{sp} - \left(1 - \frac{S}{W}\right) \alpha_{ss}}{k \alpha_{ss} + \alpha_{\delta}} \left(\frac{\Delta \lambda_{T}}{\lambda_{0T}} - \alpha_{RH} \Delta RH\right) \tag{A4}$$

This is the same relation as, in fact inspired from, [4].

Method 2

Using (A2b) from (A1b)

$$\frac{\Delta\lambda_{\varepsilon}}{\lambda_{0\varepsilon}} = k\varepsilon_{m} + \frac{k\alpha_{sp} + \alpha_{\delta} + k\alpha_{ss}\frac{S}{W}}{k\alpha_{ss} + \alpha_{\delta}} \left(\frac{\Delta\lambda_{T}}{\lambda_{0T}} - \alpha_{RH}\Delta RH\right) + \alpha_{RH}\Delta RH$$

$$\varepsilon_{m} = \frac{1}{k}\frac{\Delta\lambda_{\varepsilon}}{\lambda_{0\varepsilon}} - \frac{1}{k}\frac{k\alpha_{sp} + \alpha_{\delta} + k\alpha_{ss}\frac{S}{W}}{k\alpha_{ss} + \alpha_{\delta}} \left(\frac{\Delta\lambda_{T}}{\lambda_{0T}} - \alpha_{RH}\Delta RH\right) - \frac{1}{k}\alpha_{RH}\Delta RH$$
(A5b)

$$\varepsilon_{m} = \frac{1}{k} \frac{\Delta \lambda_{\varepsilon}}{\lambda_{0\varepsilon}} - \frac{1}{k} \frac{k \alpha_{sp} + \alpha_{\delta} + k \alpha_{ss} \overline{W}}{k \alpha_{ss} + \alpha_{\delta}} \left(\frac{\Delta \lambda_{T}}{\lambda_{0T}} - \alpha_{RH} \Delta RH \right) - \frac{1}{k} \alpha_{RH} \Delta RH$$
 (A5b)

No, if we neglect the relative humidity term and only consider it as an uncertainty source ($\delta \epsilon_{RH}$ instead of α_{RH} , see (13)), equation (A5b) becomes

$$\varepsilon_{m} = \frac{1}{k} \frac{\Delta \lambda_{\varepsilon}}{\lambda_{0\varepsilon}} - \frac{1}{k} \frac{\Delta \lambda_{T}}{\lambda_{0T}} \frac{k \alpha_{sp} + \alpha_{\delta} + k \alpha_{ss} \frac{S}{W}}{k \alpha_{ss} + \alpha_{\delta}} + \delta \varepsilon_{RH}$$
(A6)

and we have proven equation (6).

Now, if we consider non-FOBM type of sensors and discard any stud effects, we can simply put α_{ss} to zero, from (A6) we get

$$\varepsilon_{m} = \frac{1}{k} \frac{\Delta \lambda_{\varepsilon}}{\lambda_{0\varepsilon}} - \frac{1}{k} \frac{\Delta \lambda_{T}}{\lambda_{0T}} \frac{k \alpha_{sp} + \alpha_{\delta}}{\alpha_{\delta}} + \delta \varepsilon_{RH}$$

$$\varepsilon_{m} = \frac{1}{k} \frac{\Delta \lambda_{\varepsilon}}{\lambda_{0\varepsilon}} - \frac{1}{k} \frac{\Delta \lambda_{T}}{\lambda_{0T}} \left(\frac{k \alpha_{sp}}{\alpha_{\delta}} + 1 \right) + \delta \varepsilon_{RH}$$
(A7)

And we have proven equation (4).

Appendix B: Sensitivity factors

The uncertainty calculation is presented in equation (15). This equation contains various derivatives of the blade bending moment M with respect to the various uncertainty components.

The partial derivates of the strain ε with respect to the various uncertainty sources are detailed below for the various fiber optic strain sensoring

Classical, pad mounted FO

$$\varepsilon_{m} = C \left(\frac{1}{k} \frac{\Delta \lambda_{\varepsilon}}{\lambda_{0\varepsilon}} - \frac{1}{k} \frac{\Delta \lambda_{T}}{\lambda_{0T}} \left(\frac{k \alpha_{sp}}{\alpha_{\delta}} + 1 \right) \right) + \delta \varepsilon_{RH} + \delta \varepsilon_{\varepsilon T}$$

$$\Delta \lambda_{\varepsilon}: \qquad \frac{\partial \varepsilon_{m}}{\partial \Delta \lambda_{\varepsilon}} = C \frac{1}{k} \frac{1}{\lambda_{0\varepsilon}}$$

$$\Delta \lambda_{T}: \qquad \frac{\partial \varepsilon_{m}}{\partial \Delta \lambda_{T}} = C \frac{1}{k} \frac{1}{\lambda_{0T}} \left(\frac{k \alpha_{sp}}{\alpha_{\delta}} + 1 \right)$$

$$k: \qquad \frac{\partial \varepsilon_{m}}{\partial k} = \frac{C}{k^{2}} \frac{\Delta \lambda_{\varepsilon}}{\lambda_{0\varepsilon}} + \frac{C}{k^{2}} \frac{\Delta \lambda_{T}}{\lambda_{0T}}$$

$$\alpha_{sp}: \qquad \frac{\partial \varepsilon_{m}}{\partial \alpha_{sp}} = -C \frac{\Delta \lambda_{T}}{\lambda_{0T}} \frac{1}{\alpha_{\delta}}$$

$$\alpha_{\mathcal{S}}: \qquad \frac{\partial \varepsilon_{m}}{\partial \alpha_{\delta}} = C \frac{\Delta \lambda_{T}}{\lambda_{0T}} \frac{\alpha_{sp}}{\alpha_{\delta}^{2}}$$

$$\delta \varepsilon_{RH}: \qquad \frac{\partial \varepsilon_{m}}{\partial \delta \varepsilon_{RH}} = 1$$

$$\delta \varepsilon_{\varepsilon T}: \qquad \frac{\partial \varepsilon_{m}}{\partial \delta \varepsilon_{\varepsilon T}} = 1$$

$$\lambda_{0\varepsilon}: \qquad \frac{\partial \varepsilon_{m}}{\partial \lambda_{0\varepsilon}} = \frac{C}{k} \frac{\Delta \lambda_{\varepsilon}}{\lambda_{0\varepsilon}^{2}}$$

$$\lambda_{0T}: \qquad \frac{\partial \varepsilon_{m}}{\partial \lambda_{0T}} = -\frac{C}{k} \frac{\Delta \lambda_{T}}{\lambda_{0T}^{2}} \left(\frac{k \alpha_{sp}}{\alpha_{\delta}} + 1 \right)$$

Temperature calibrated, pad mounted FO

$$\varepsilon_{m} = C \left(\frac{1}{k} \frac{\Delta \lambda_{\varepsilon}}{\lambda_{0\varepsilon}} - \Delta T \left(\frac{\alpha_{\delta}}{k} + \alpha_{sp} \right) \right) + \delta \varepsilon_{RH} + \delta \varepsilon_{\varepsilon T}$$

$$\Delta \lambda_{\varepsilon}: \qquad \frac{\partial \varepsilon_{m}}{\partial \Delta \lambda_{\varepsilon}} = \frac{c}{k} \frac{1}{\lambda_{0\varepsilon}}$$

$$\Delta T: \qquad \frac{\partial \varepsilon_{m}}{\partial \Delta T} = -C \left(\frac{\alpha_{\delta}}{k} + \alpha_{sp} \right)$$

$$k: \qquad \frac{\partial \varepsilon_{m}}{\partial k} = -\frac{c}{k^{2}} \frac{\Delta \lambda_{\varepsilon}}{\lambda_{0\varepsilon}} + \frac{c}{k^{2}} \Delta T \alpha_{\delta}$$

$$\alpha_{sp}: \qquad \frac{\partial \varepsilon_{m}}{\partial \alpha_{sp}} = -C * \Delta T$$

$$\alpha_{\delta}: \qquad \frac{\partial \varepsilon_{m}}{\partial \alpha_{\delta}} = -C \frac{\Delta T}{k}$$

$$\delta \varepsilon_{RH}: \qquad \frac{\partial \varepsilon_{m}}{\partial \delta \varepsilon_{RH}} = 1$$

$$\delta \varepsilon_{\varepsilon T}: \qquad \frac{\partial \varepsilon_{m}}{\partial \delta \varepsilon_{\varepsilon T}} = 1$$

FOBM

$$\varepsilon_{m} = C \left(\frac{1}{k} \frac{\Delta \lambda_{\varepsilon}}{\lambda_{0\varepsilon}} - \frac{1}{k} \frac{\Delta \lambda_{T}}{\lambda_{0T}} \left(\frac{k\alpha_{sp} + \alpha_{\delta} + k\alpha_{ss} \frac{S}{W}}{k\alpha_{ss} + \alpha_{\delta}} \right) \right) + \delta \varepsilon_{RH} + \delta \varepsilon_{\varepsilon T}$$

$$\Delta \lambda_{\varepsilon}: \qquad \frac{\partial \varepsilon_{m}}{\partial \Delta \lambda_{\varepsilon}} = C \frac{1}{k} \frac{1}{\lambda_{0\varepsilon}}$$

$$\Delta \lambda_{T}: \qquad \frac{\partial \varepsilon_{m}}{\partial \Delta \lambda_{T}} = -C \frac{1}{k} \frac{1}{\lambda_{0T}} \left(\frac{k\alpha_{sp} + \alpha_{\delta} + k\alpha_{ss} \frac{S}{W}}{k\alpha_{ss} + \alpha_{\delta}} \right)$$

$$\begin{array}{lll} \mathsf{K}: & \frac{\partial \varepsilon_m}{\partial \mathsf{k}} = -\frac{C}{k^2} \frac{\Delta \lambda_{\varepsilon}}{\lambda_{0\varepsilon}} + \frac{C}{k^2} \frac{\Delta \lambda_T}{\lambda_{0T}} \frac{\left(k \alpha_{SS} \left(2 \alpha_{\delta} + k \alpha_{Sp} + k \alpha_{SS} \frac{S}{W}\right) + \alpha_{\delta}^2\right)}{\left(k \alpha_{SS} + \alpha_{\delta}\right)^2} \\ \mathsf{C}_{Sp}: & \frac{\partial \varepsilon_m}{\partial \alpha_{Sp}} = -C \frac{\Delta \lambda_T}{\lambda_{0T}} \frac{1}{k \alpha_{SS} + \alpha_{\delta}} \\ \mathsf{C}_{S}: & \frac{\partial \varepsilon_m}{\partial \alpha_{\delta}} = C \frac{\Delta \lambda_T}{\lambda_{0T}} \frac{\left(\alpha_{Sp} - \left(1 - \frac{S}{W}\right) \alpha_{SS}\right)}{\left(k \alpha_{SS} + \alpha_{\delta}\right)^2} \\ \mathsf{C}_{SS}: & \frac{\partial \varepsilon_m}{\partial \alpha_{SS}} = C \frac{\Delta \lambda_T}{\lambda_{0T}} \frac{\left(k \alpha_{Sp} + \left(1 - \frac{S}{W}\right) \alpha_{\delta}\right)}{\left(k \alpha_{SS} + \alpha_{\delta}\right)^2} \\ \mathsf{S}: & \frac{\partial \varepsilon_m}{\partial S} = -C \frac{\Delta \lambda_T}{\lambda_{0T}} \frac{1}{k \alpha_{SS} + \alpha_{\delta}} \frac{\alpha_{SS}}{W} \\ \mathsf{W}: & \frac{\partial \varepsilon_m}{\partial W} = -C \frac{\Delta \lambda_T}{\lambda_{0T}} \frac{1}{k \alpha_{SS} + \alpha_{\delta}} \frac{S \alpha_{SS}}{W^2} \\ \mathsf{\delta}_{\mathcal{E}_{RH}}: & \frac{\partial \varepsilon_m}{\partial \delta \varepsilon_{RH}} = 1 \\ \mathsf{\delta}_{\mathcal{E}_{\mathcal{E}_{\mathcal{T}}}:} & \frac{\partial \varepsilon_m}{\partial \delta \varepsilon_{ET}} = 1 \\ \lambda_{0\varepsilon}: & \frac{\partial \varepsilon_m}{\partial \lambda_{0\varepsilon}} = -\frac{C}{k} \frac{\Delta \lambda_{\varepsilon}}{\lambda_{0\varepsilon}^2} \\ \lambda_{0T}: & \frac{\partial \varepsilon_m}{\partial \lambda_{0T}} = \frac{C}{k} \frac{\Delta \lambda_T}{\lambda_{0T}^2} \left(\frac{k \alpha_{Sp} + \alpha_{\delta} + k \alpha_{SS} \frac{S}{W}}{k \alpha_{SS} + \alpha_{\delta}}\right) \end{array}$$